ACS Sustainable Chemistry & Engineering

pubs.acs.org/journal/ascecg

Research Article

Termite Gut Microbiota Contribution to Wheat Straw Delignification in Anaerobic Bioreactors

Louison Dumond, Pui Ying Lam, Gijs van Erven, Mirjam Kabel, Fabien Mounet, Jacqueline Grima-Pettenati, Yuki Tobimatsu, and Guillermina Hernandez-Raquet*

Cite This: *ACS Sustainable Chem. Eng.* 2021, 9, 2191−2202

Read Online

ACCESS | Metrics & More | Article Recommendations | Supporting Information

ABSTRACT: Lignin is a major lock for lignocellulose valorization in biorefineries, prompting a need to find new ligninolytic systems. Termites are efficient lignocellulose degraders, and a large part of this ability comes from its anaerobic gut microbiome. However, the potential of termite gut microbiomes to degrade lignin under anaerobic conditions has yet to be elucidated. By applying wet chemistry, multidimensional NMR spectroscopy, and quantitative ^{13}C-IS py-GC-MS, we determined the chemical and structural characteristics of wheat straw digested by the gut microbiomes of higher termites *Nasutitermes ephratae*, *Nasutitermes lujae*, *Microcerotermes parvus*, and *Termes hospes* implemented in anaerobic bioreactors. Interestingly, all gut microbiomes managed to remove lignin (up to 37%), although hemicellulose (mean 51%) and cellulose (mean 41%) were degraded more efficiently. Important structural differences, indicative of ligninolytic action, were discerned in the residual lignin. For the studied termite gut microbiomes, a slight decrease of S/G ratio was observed upon digestion, whereas lignin's interunit linkages and Cα-oxidized moieties, including benzaldehyde and hydroxypropiovanillone/syringone substructures, accumulated. Additionally, tricin terminal units were clearly depleted, along with decreases in *p*-coumarate and ferulate pendant units. At least 80% of the observed delignification is estimated to be due to the removal of "true" lignin, with the remainder being explained by the removal of hydroxycinnamic acids and tricin. Collectively, our findings suggest a partial deconstruction of lignin, with "peripheral" lignin subunits being preferentially targeted. The present work thus provides new insights into the anaerobic deconstruction of lignin by termite gut microbiomes.

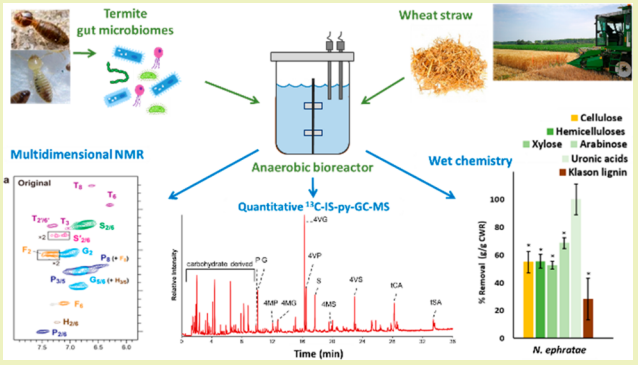

KEYWORDS: *Lignin, Lignocellulose, Termite gut microbiome, NMR spectroscopy, py-GC-MS, Delignification, Anaerobic digestion*

INTRODUCTION

The increasing global demand for producing energy, transportation fuels, and sustainable commodity chemicals from nonfood renewable resources has motivated the development of lignocellulose biorefineries.[1] However, lignocellulosic biomass is highly resistant against bioconversion that can largely be ascribed to the recalcitrance of the polymers it contains.

Lignocellulosic biomass consists mainly of the three polymers, cellulose, hemicelluloses, and lignin, of which the former two are polysaccharides, and the latter is an aromatic polymer. These polymers are elaborately interwoven with each other to form a complex three-dimensional structure and constitute the majority of the lignocellulosic agricultural residues, accounting for 30−50% (cellulose), 20−30% (hemicelluloses), and 15−30% (lignin) of the dry matter.[2,3] The composition of the biomass is completed by ash, proteins, and wax.

Lignin plays a key role in plants as it provides mechanical strength and protection against environmental and microbial attacks.[4] While lignin, therefore, forms the main recalcitrant factor against polysaccharide conversion in biorefinery approaches,[5] it is also the most abundant natural renewable source of aromatic compounds for chemical industries. These features have prompted a multitude of research efforts into lignin degradation, with biological conversion strategies increasingly receiving attention.[5]

Lignin is mainly synthesized from three monolignols, namely, *p*-coumaryl alcohol, coniferyl alcohol, and sinapyl alcohol, which, respectively, give rise to the three major phenylpropane units, *p*-hydroxyphenyl (H), guaiacyl (G), and syringyl (S) units, when incorporated into the lignin polymer.[6] In monocotyledonous grass species, including wheat, lignin

Received: October 25, 2020
Revised: December 29, 2020
Published: January 25, 2021

https://dx.doi.org/10.1021/acssuschemeng.0c07817
ACS Sustainable Chem. Eng. 2021, 9, 2191−2202

additionally contains γ-*p*-coumaroylated G and S units derived from polymerization of γ-*p*-coumaroylated monolignols, and also tricin units derived from polymerization of a flavone tricin.[6] In addition, (di)ferulates (FA), mainly ester-linked to hemicelluloses (glucuronoarabinoxylans, GAX), are partially bonded to lignin in grass cell walls.[6,7]

Despite lignin's recalcitrance to biodegradation, in nature, diverse microorganisms have shown to be able to degrade lignin, with white-rot like *Phanerochaete chrysosporium* and *Trametes versicolor* which have been applied for biotechnological purposes.[8] Compared to fungi, bacteria display lower ligninolytic activities, but their versatile metabolisms enable them to degrade a large variety of lignin-derived aromatic compounds.[9] Furthermore, bacterial enzymes are relatively easily produced, especially given the genetic tools for their heterologous overexpression;[10] therefore, several research teams are aiming to decipher bacterial lignin degradation.

Lignin degradation by bacteria was first suggested in Actinomycetes from the genus *Streptomyces*.[11] Since then, the ligninolytic capacity of *Streptomyces* has been deeply characterized,[12,13] and members of *Pseudomonas*, *Rhodococcus*, *Bacillus*, and *Acinetobacter* have been described as potential ligninolytic bacterial species.[14] Nevertheless, the lignin degradation capacity of bacteria associated with the partial or strict anaerobic digestive system of herbivorous animals, such as ruminants and phytophagous insects in which overcoming lignin recalcitrance might play an important role, still largely remains to be elucidated. These organisms, therefore, might harbor interesting bacterial species.

Of these phytophagous insects, termites are among the most efficient lignocellulose decomposers,[15] with high potential for lignocellulose biorefinery applications. Termites are historically classified into higher and lower termites depending on their lignocellulose degradation mechanisms. In lower termites, most of the lignocellulose degradation comes from the interaction of the termite with flagellated protists as well as prokaryotes constituting their gut microbiome. While higher termites lack flagellated protists, they shelter a variety of lignocellulolytic prokaryotes within their gut. Some higher termites also recruit ectosymbiotic fungi for efficient lignocellulose degradation.[15]

While the degradation of the cell wall polysaccharides in termites has been extensively documented in the literature,[15] it is still controversial how termites overcome the lignin barrier. Initially, it was hypothesized that there was no lignin degradation in termites at all, the activity of termites being limited to the degradation of mono- or dimeric-lignin model compounds.[16,17] With the advancement of tools for lignin analysis, especially the use of multidimensional nuclear magnetic resonance (NMR) techniques,[18,19] polymeric lignin degradation by termites has been recently reassessed.[20,21] For instance, a recent study which employed two-dimensional (2D) heteronuclear single quantum coherence (HSQC) NMR for dissecting lignocellulose decomposition by a lower termite *Coptotermes formosanus* provided NMR signatures supporting that lignin polymers can be at least partially decomposed during their passage through the termite gut digestive system.[20] Similarly, studies employing pyrolysis coupled to gas chromatography with mass spectrometric detection (py-GC-MS) reported structural modifications of lignin albeit with no clear depolymerization of lignin polymer backbones by lower termites *Cryptotermes brevis* and *C. formosanus*.[22,23] Recently, the lignin analysis toolkit has been further advanced by the development of a py-GC-MS method that employs uniformly ^{13}C-labeled lignin as internal standard, allowing quantitative analysis of lignin content and structure.[24] Proven invaluable for the analysis of fungal ligninolysis, this method might provide additional insights into lignin degradation by termites.[25]

In a previous work we reported the lignocellulose degradation by gut microbiomes of four higher termite species *Nasutitermes ephratae*, *Nasutitermes lujae*, *Microcerotermes parvus*, and *Termes hospes*. These microbiomes were grown on lignocellulosic biomass in anaerobic bioreactors, demonstrating their high potential to convert lignocellulosic substrates into carboxylates.[26] In this study, we aimed to decipher lignin modification induced by termite gut microbiomes by expanding upon our previous work, using the resulting digested wheat straw to assess lignocellulose modifications by making use of in-depth structural analysis (whole-cell wall HSQC NMR and ^{13}C-IS py-GC-MS), complemented by wet chemistry.

EXPERIMENTAL SECTION

Lignocellulose Degradation by Termite Gut Inocula in Anaerobic Bioreactors. The lignocellulose degradation capacity of gut microbiomes from four different species of higher termites *Microcerotermes parvus*, *Termes hospes*, *Nasutitermes ephratae*, and an undescribed species closely related to *N. lujae* (herein after *N. lujae*) was assessed in anaerobic bioreactors (Applikon MiniBio 500). Termite guts (500 guts) were used as inocula for two replicate anaerobic bioreactors for each termite species, using a minimal medium and autoclaved (121 °C, 20 min, 1.2 bar) milled wheat straw as the sole carbon source as previously described[26] and detailed in the Supporting Information (Materials and Methods section in Supporting Information). At the end of the 20 days of incubation, VFA and gas production were determined, and the whole culture broth was snap frozen in liquid nitrogen and kept at −80 °C until further use. For chemical characterization, replicate samples were pooled together.

Volatile Fatty Acid Quantification. Volatile fatty acids (VFAs) contained in the liquid phase of samples were analyzed using a Varian 3900 gas chromatograph equipped with a flame ionization detector and CP-Wax 58 (FFAP) CB column as described previously.[27]

Volatile Solid Quantification. Wheat straw concentration was determined at the beginning and at the end of the 20 day incubation by measuring the total (TS) and volatile (VS) solids, corresponding to the solid organic fraction (for details, see the Supporting Information).

Cell Wall Extraction and Grinding. Extractive-free cell wall residues (CWRs) were obtained by sonication-solvent extraction of 2 g of wheat straw samples.[19] CWR was obtained after drying at room temperature overnight and for 24 h at 55 °C. CWR was then milled in a MM 400 ball mill (Retsch) (Supporting Information).

Polysaccharide Analysis and Klason Lignin Determination. Wheat straw composition was determined on the original wheat straw and the digested samples collected from the bioreactors at the end of the incubation period. Their chemical composition was determined using the sulfuric acid hydrolysis method described by Lazuka et al.[28] (Supporting Information). The insoluble residue was washed with distilled water and dried at 105 °C overnight to determine Klason lignin content. Sugar composition was determined on an Ultimate 3000 Dionex HPLC instrument with refractive index detector (Thermo Scientific) equipped with a BioRad Aminex HPX 87H affinity column.[28]

To estimate the absolute extent of removal of the different lignocellulose components by the gut microbiomes in the bioreactor experiments, we computed the total remaining mass of polymers (m_p) (Figure 1) per liter as such:

$$m_p = w_p \times m_{VS} \times \frac{m_{CWR}}{m_t} \quad (1)$$

https://dx.doi.org/10.1021/acssuschemeng.0c07817
ACS Sustainable Chem. Eng. 2021, 9, 2191−2202

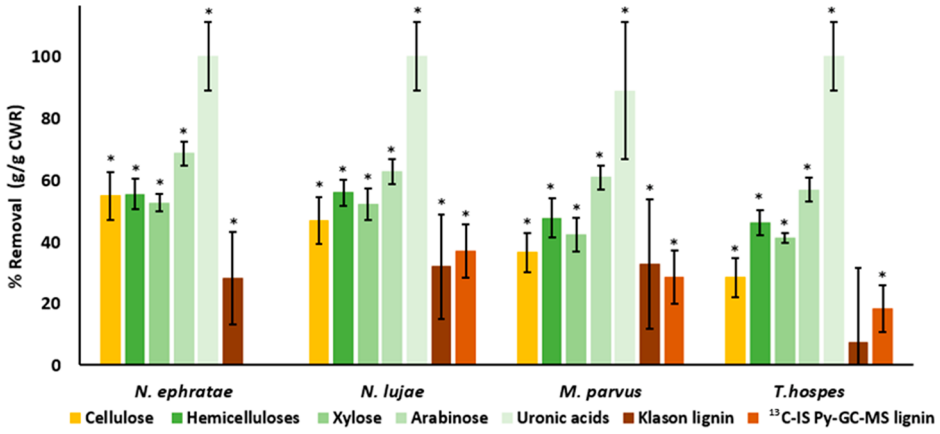

Figure 1. Estimation of absolute lignocellulose compositional changes of wheat straw samples digested by gut microbiomes based on volatile solid loss and chemical composition analysis of the digested residues. Average values and the standard deviation are expressed as the percentage change compared to undigested original wheat straw (g/100 g CWR), with hemicellulose being the sum of xylose, arabinose, and uronic acids. Statistical differences are marked with * ($p < 0.05$, $n = 3$, Student's t-test). ^{13}C-IS py-GC-MS lignin removal was not measured for *N. ephratae* because of the lack of sample.

Table 1. Volatile Solids (VS) Content and Volatile Fatty Acid (VFA) Production after 20 days of Incubation in Anaerobic Bioreactors[a]

		digested wheat straw			
		gut microbe origin:			
	undigested original wheat straw	*N. ephratae*	*N. lujae*	*M. parvus*	*T. hospes*
VS content (g/L)	18.84	10.31 ± 0.91	11.30 ± 0.83	12.81 ± 0.91	12.81 ± 0.70
VFA production (g/L)	0.32	5.61	3.99	3.46	3.49

[a]Adapted from Auer et al.[26] Values are expressed as means ± SD ($n = 3$).

considering the mass percentage of said polymers (w_p) (Table 2), total mass of volatile solids (VS) remaining in the bioreactors (m_{VS}) (Table 1) corrected by weight loss induced by extraction $\left(\frac{m_{CWR}}{m_t}\right)$.

Thioacidolysis. Analytical thioacidolysis was performed according to Méchin et al.[29] (Supporting Information). Trimethylsilylated lignin-derived monomers were quantified on a Trace1300 GC/MS instrument (Thermoscientific) equipped with a Triple Quadripole-Ion trap and an Agilent DB-5 column (Agilent Technologies).[30]

2D HSQC NMR. CWR samples were swelled in DMSO-d_6/pyridine-d_5 (4:1, v/v) for the gel-state NMR analysis as described previously.[20] NMR spectra were acquired using the Avance III 800US system (Bruker Biospin, Billerica, MA) equipped with a cryogenically cooled 5 mm TCI gradient probe (Bruker Biospin). 2D HSQC NMR experiments were carried out using the standard Bruker implementation ("hsqcetgpsp.3") with the parameters described in the literature.[18,19] Data processing and analysis were performed using TopSpin 4.0 software (Bruker Biospin) as described previously.[31,32] The central DMSO-d_6 solvent peaks (δ_C/δ_H: 39.5/2.49 ppm) were used as internal references. For volume integration analysis of the aromatic contour signals, C_2−H_2 correlations from G, G′, and F, C2−H2/C6−H6 correlations from S, S′, and P, and C2′−H2′/C6′−H6′ correlations from T were manually integrated, and S, S′, P, and T integrals were logically halved. For the polysaccharide anomeric signals, C1−H1 correlations from Gl, X, X′, X″, X‴, A, and U were integrated. For the lignin side-chain signals, Cα−Hα correlations from I, II, III, III′, and IV″, Cγ−Hγ correlations from IV‴, and Cγ−Hγ correlations from IV and IV′ were integrated, and III, III′, IV, and IV‴ integrals were logically halved. The obtained integration values were normalized on a $1/2S_{2/6} + 1/2S'_{2/6} + G_2 + G'_2 + 1/2H'_{2/6} = 100$ basis for each spectrum.

Quantitative py-GC-MS with ^{13}C Lignin as the Internal Standard. Analytical pyrolysis coupled to gas chromatography with high-resolution mass spectrometric detection (Exactive Orbitrap, Thermo Scientific, Waltham, MA) was performed as previously described.[33] To each CWR sample (~80 μg), 10 μL of a ^{13}C wheat straw lignin internal standard (IS) solution (1 mg mL^{-1} ethanol/chloroform 50:50 v/v) was added and dried prior to analysis. All samples were prepared and analyzed in triplicate. Lignin-derived pyrolysis products were monitored in full MS mode on the most abundant fragment per compound (both nonlabeled and uniformly ^{13}C labeled). Pyrograms were processed by TraceFinder 4.0 software. Lignin contents and relative abundances of lignin-derived pyrolysis products were calculated as described previously.[33]

Statistical Analysis. Statistical differences between digested and undigested samples were calculated with a t-test, $p < 0.05$, n = number of samples.

RESULTS

Wheat Straw Degradation by Termite Gut Microbiomes in Anaerobic Bioreactors. Wheat straw biomass was incubated for 20 days in anaerobic bioreactors inoculated with gut microbiomes from higher termites, *N. ephratae*, *N. lujae*, *M. parvus*, and *T. hospes*.[26] To assess the degradation of wheat straw biomass, total volatile solid (VS) content and volatile fatty acid (VFA) production were determined (Table 1). Regardless of the gut microbiome origins, wheat straw was clearly degraded as determined by the loss of VS, but the extent was different between the gut microbiome origins. The highest degradation rate (%, w/w) was observed for the gut microbiome of *N. ephratae* (45.2 ± 5.0%), followed by those of *N. lujae* (37.1 ± 4.3%), *M. parvus* (31 ± 3.7%), and *T. hospes* (30 ± 5.0%). Wheat straw in the bioreactors was mainly transformed into VFA, with *N. ephratae* being the best VFA producer. VFA composition was dominated by acetate (>85%) and completed by propionate and butyrate.[26]

https://dx.doi.org/10.1021/acssuschemeng.0c07817
ACS Sustainable Chem. Eng. 2021, 9, 2191−2202

Table 2. Lignocellulose Compositional Analysis of Wheat Straw Samples Digested by Gut Microbiomes from Four Higher Termites in Anaerobic Bioreactors[a]

		digested wheat straw			
		gut microbe origin:			
	undigested original wheat straw	*N. ephratae*	*N. lujae*	*M. parvus*	*T.hospes*
cellulose (g/100 g CWR)	43.3 ± 2.2	38.4 ± 2.2 (−11.3%)	43.1 ± 2.3 (−0.5%)	45.4 ± 1.1 (+4.8%)	44.2 ± 0.6 (−2%)
		Hemicelluloses (g/100 g CWR)			
total	34.2 ± 1.7	29.9 ± 0.6* (−12.5%)	28.3 ± 0.4* (−17.3%)	29.6 ± 0.7* (−13.4%)	26.3 ± 0.6* (−23.1%)
xylose	31.2 ± 1.5	29.6 ± 1.2 (−5.1%)	27.0 ± 1.1* (−13.5%)	28.5 ± 0.1* (−8.7%)	25.0 ± 0.6* (−19.9%)
arabinose	3.5 ± 0.3	2.0 ± 0.1* (−42.9%)	2.0 ± 0.1* (−42.9%)	2.0 ± 0.1* (−42.9%)	1.9 ± 0.1* (−45.7%)
uronic acid	0.6 ± 0.0	ND[b] (−100%)	0.1 ± 0.1 (−83.3%)	ND (−100%)	ND (−100%)
		Lignin (g/100 g CWR)			
by Klason	22.5 ± 3.2	31.7 ± 1.3* (+40.0%)	28.6 ± 4.1* (+27.0%)	25.0 ± 3.4 (+11.0%)	29.6 ± 4.6 (+31.5%)
by ^{13}C-IS py-GC-MS	24.2 ± 1.4	NA[c]	28.6 ± 1.5* (+18.2%)	28.6 ± 1.3* (+18.2%)	28.1 ± 0.8* (+16.0%)

[a]Values are expressed as means ± SD g per 100 g cell wall residues (CWRs). Values in parentheses indicate percentage change compared to undigested original wheat straw. Statistical differences are marked with * ($p < 0.05$, $n = 3$, Student's *t*-test). [b]ND: not detected. [c]NA: not analyzed.

Lignocellulose Compositional Changes in Wheat Straw Degradation by Termite Gut Microbiomes in Anaerobic Bioreactors. To gain insights into the mechanisms underlying conversions of lignocellulose components by termite gut microbiomes, the samples of cell wall residue (CWR) prepared from the undigested and digested wheat straws were chemically characterized. The changes in lignocellulose composition were determined by sugar analysis and lignin content analysis based on Klason lignin and ^{13}C-IS py-GC-MS approaches (Table 2). Sugar analysis showed slight decreases in cellulose content only in wheat straw CWR digested by the *N. ephratae* gut microbiome, whereas apparent cellulose content remained unchanged in the CWR samples digested by the microbes from *N. lujae* and *T. hospes*, or slightly increased in the CWR samples digested by the *M. parvus* microbiome.

In contrast, a decrease in the hemicellulose fraction was observed for all the digested samples, ranging from 12.5% to 23% compared to the initial hemicellulose content of undigested, original wheat straw. Within the hemicellulose fraction, xylose content was reduced by 5−20%, whereas arabinose content was more drastically reduced by ∼50%, in all the digested samples. In addition, uronic acid content in the digested samples decreased by more than 80% in all the digested samples. Thus, GAX fractions were preferentially removed by the microbiomes action.

The lignin content in wheat straw samples was assessed by either or both Klason and ^{13}C-IS py-GC-MS (Table 2). The two methods provided overall similar lignin content data, with the ^{13}C-IS py-GC-MS method being superior in precision (RSD < 6%), and consistently showed increases of lignin in all the digested samples compared to the original wheat straw. The increment measured by the Klason method ranged from 11% to 40% with statistical significance for the samples digested by the gut microbiomes from *N. ephratae* (+40%) and *N. lujae* (+27%) ($p < 0.05$). A more conservative increment was measured by py-GC-MS, varying between 16% and 18% with statistical significance for all the digested samples. Collectively, these data show that, for all the termite gut inocula studied, there is a preferential degradation of the hemicellulose fraction, particularly GAX, over cellulose and lignin fractions.

Furthermore, the absolute extent of removal of each lignocellulose fraction by the gut microbiomes was estimated based on the VS loss (Table 1) and wheat straw chemical composition (Table 2) (see the Material and Methods section in the Supporting Information). This analysis showed a higher removal of polysaccharides by the *N. ephratae* gut microbiome compared to other species, with a 55% loss of both cellulose and hemicellulose fractions (Figure 1). Other termite microbiomes also displayed efficient polysaccharide removal with cellulose degradation ranging from 28% to 47% and hemicellulose degradation ranging from 46% to 55%. Notably, all the termite gut microbiomes displayed higher or at least similar hemicellulose consumption compared to cellulose. Whereas both *Nasutitermes* (*N. ephratae* and *N. lujae*) gut microbiomes removed similar amounts of cellulose and hemicelluloses, microbiomes from *M. parvus* and *T. hospes* displayed a preferential degradation toward hemicelluloses as compared to that toward cellulose. Within the hemicellulose fraction, arabinosyl and uronosyl moieties seemed to be more easily degraded than xylosyl moieties.

Even though the digested wheat straw residues were enriched in lignin content (Table 2), in fact, significant amounts of lignin appeared to be removed (Figure 1). The Klason lignin assay suggested that 28−32% of lignin in the original wheat straw was removed by *N. ephratae*, *N. lujae*, and *M. parvus* gut inocula, whereas a nonsignificant lignin removal (7%) was found for *T. hospes*. The corresponding values quantified by py-GC-MS were in a similar order of magnitude for *N. lujae* and *M. parvus*; in contrast, *T. hospes* displayed a lignin degradation of 18% ($p < 0.05$), higher than that estimated by the Klason method. Given the accuracy for lignin quantification of the py-GC-MS method over that of the Klason methodology, we imply that also *T. hospes* is able to remove lignin.

Structural Characterization of Digested Wheat Straw Residues by Thioacidolysis, 2D HSQC NMR, and ^{13}C-IS

https://dx.doi.org/10.1021/acssuschemeng.0c07817
ACS Sustainable Chem. Eng. 2021, 9, 2191−2202

Table 3. Thioacidolysis-Based Lignin Compositional Analysis of Cell Wall Residues from Wheat Straw Digested by Termite Gut Microbiomes[a]

		digested wheat straw		
		gut microbe origin		
	undigested original wheat straw	*N. lujae*	*M. parvus*	*T. hospes*
		Monomer Yield (μmol/g Klason Lignin)		
G	429 ± 41	326 ± 46* (−24%)	544 ± 121 (21%)	446 ± 63 (4%)
S	543 ± 90	380 ± 46* (−30%)	592 ± 186 (9%)	423 ± 58 (−22%)
G + S	972 ± 132	706 ± 63* (−27%)	1133 ± 303 (17%)	871 ± 107 (−11%)
		Monomer Yield (μmol/g py-GC-MS Lignin)		
G	400 ± 38	326 ± 46 (−19%)	476 ± 106 (16%)	504 ± 57 (20%)
S	504 ± 84	380 ± 46 (−25%)	517 ± 162 (3%)	480 ± 64 (−5%)
G + S	904 ± 122	706 ± 63 (−22%)	993 ± 268 (+10%)	984 ± 118 (9%)
		Monomer Ratio (mol/mol)		
S/G	1.28 ± 0.06	0.86 ± 0.08* (−33.3%)	1.08 ± 0.10* (−15.6%)	0.96 ± 0.05* (−25%)

[a]Values in parentheses indicate percentage change compared to undigested wheat straw. Statistical differences are marked with * ($p < 0.05$, $n = 3$, Student's *t*-test).

py-GC-MS. To investigate the lignin-unlocking mechanisms of termite gut microbiomes, lignocellulose structures of the original and digested wheat straw CWR samples were further characterized by thioacidolysis, 2D HSQC NMR, and ^{13}C-IS py-GC-MS, focusing on the analysis of lignin chemical structures. Due to the limited sample availability of the wheat straw samples digested by *N. ephratae* gut microbes, we report the results obtained for digestion with gut microbiomes from *N. lujae*, *M. parvus*, and *T. hospes*.

Thioacidolysis. To investigate lignin compositional change before and after the microbial digestion of wheat straw, we performed analytical thioacidolysis, which quantifies lignin-derived monomers released by the chemical cleavage of β−O−4 linkages, the major intermonomeric linkage type in lignin polymer.[34] Since grass lignins are mainly constituted of G and S units, typically with only a minor fraction of H units[6,35] (as also confirmed by 2D NMR and py-GC-MS below), we only quantified G and S monomers in the present analysis. The total G + S monomer yield based on lignin content was somehow decreased in the CWR samples digested by the *N. lujae* microbe, whereas those determined for samples digested by *M. parvus* and *T. hospes* microbes were overall similar, compared to the undigested wheat straw, though it must be noted that substantial standard deviations were observed (Table 3). An implication for lignin modification by the action of gut microbes was deduced from the changes in S/G monomer ratio (Table 3). For all three termite gut microbiomes tested, the S/G ratio appeared to significantly decrease after digestion, suggesting a preferential degradation and/or modification of S over G units in lignin β−O−4 units as further demonstrated by NMR and py-GC-MS below.

2D HSQC NMR. 2D HSQC NMR was employed to obtain further detailed information on the chemical structures of the wheat straw cell walls digested by the termite gut microbiomes. To gain a global picture of structural alterations in both lignin and polysaccharide fractions, we collected HSQC spectra of the whole CWR samples via the direct dissolution/swelling method using the DMSO-d_6/pyridine-d_5 solvent system.[18,19] The NMR spectrum of the original, undigested wheat straw cell walls displayed major lignin and polysaccharide signals typical for grass cell walls (Table S1). The aromatic subregion (Figure 2a, Table S1) showed resolved signals from typical S, G, and H lignin aromatic units (S, S′, G, G′, and H) and grass-specific cell wall components such as tricin (T) and *p*-coumarates (P)[36] both of which are majorly bound to lignin,[36−38] and also ferulates (F) mainly bound to GAX.[7] The polysaccharide anomeric subregion (Figure 2b, Table S1) displayed anomeric signals associated with cellulose and hemicelluloses, such as those from glucans (Gl), unacetylated (X) and acetylated (X′, X″, and X‴) xylans, arabinan (A), and glucuronan (U).[18,20,25]

Furthermore, the oxygenated aliphatic and aldehyde subregions displayed signals from various intermonomeric linkage types, such as β−O−4 (I), β−5 (II), and β−β (III and III′) linkages, as well as polymer end-units, such as cinnamyl alcohol (IV), cinnamaldehyde (IV′), and benzaldehyde (IV″) end-units, in the lignin polymer backbones (Figure 3, Table S1).[18,39]

The compositional changes in the wheat straw cell walls before and after termite microbiome digestion were deduced by comparing the volume integrations of the HSQC contour signals. For a comparison between the original and digested cell wall NMR spectra, major lignin aromatic and polysaccharide anomeric signals were integrated and normalized based on the sum of the total of major lignin aromatic signals ($S_{2/6} + S'_{2/6} + G_2 + G'_2 + H_{2/6}$) (Figure 2c). Glucan (Gl) and xylan (X, X′, X″, and X‴) were the predominant polysaccharide signals detected in all the cell wall spectra (Figure 2a) and reflect the proportional changes of cellulose and hemicellulosic arabinoxylans in cell walls, respectively. Glucan signals from crystalline cellulose, however, are substantially underestimated by the current gel-state NMR method due to its incomplete gelation in the solvent.[18,19] Regardless of the termite gut microbiome tested, slight increases of glucan (Gl) signals and decreases of signals from nonacetylated and monoacetylated xylan (X, X′, and X″) and arabinan (A) were prominent after digestion (Figure 2c). This result further corroborates the preferential degradation of GAX over cellulose and lignin by the termite gut microbiomes as determined earlier by the wet-chemical analyses (Tables 2 and 3). In contrast to clear depletions in nonacetylated and monoacetylated xylan (X, X′, and X″) and arabinan (A) signals, 2,3-di-*O*-acetylated xylan (X‴) and ferulate (F) signals appeared to be rather similar between all the digested and undigested control cell wall spectra (Figure 2c), suggesting that heavily acetylated xylan and feruloylated arabinan moieties in

https://dx.doi.org/10.1021/acssuschemeng.0c07817
ACS Sustainable Chem. Eng. 2021, 9, 2191−2202

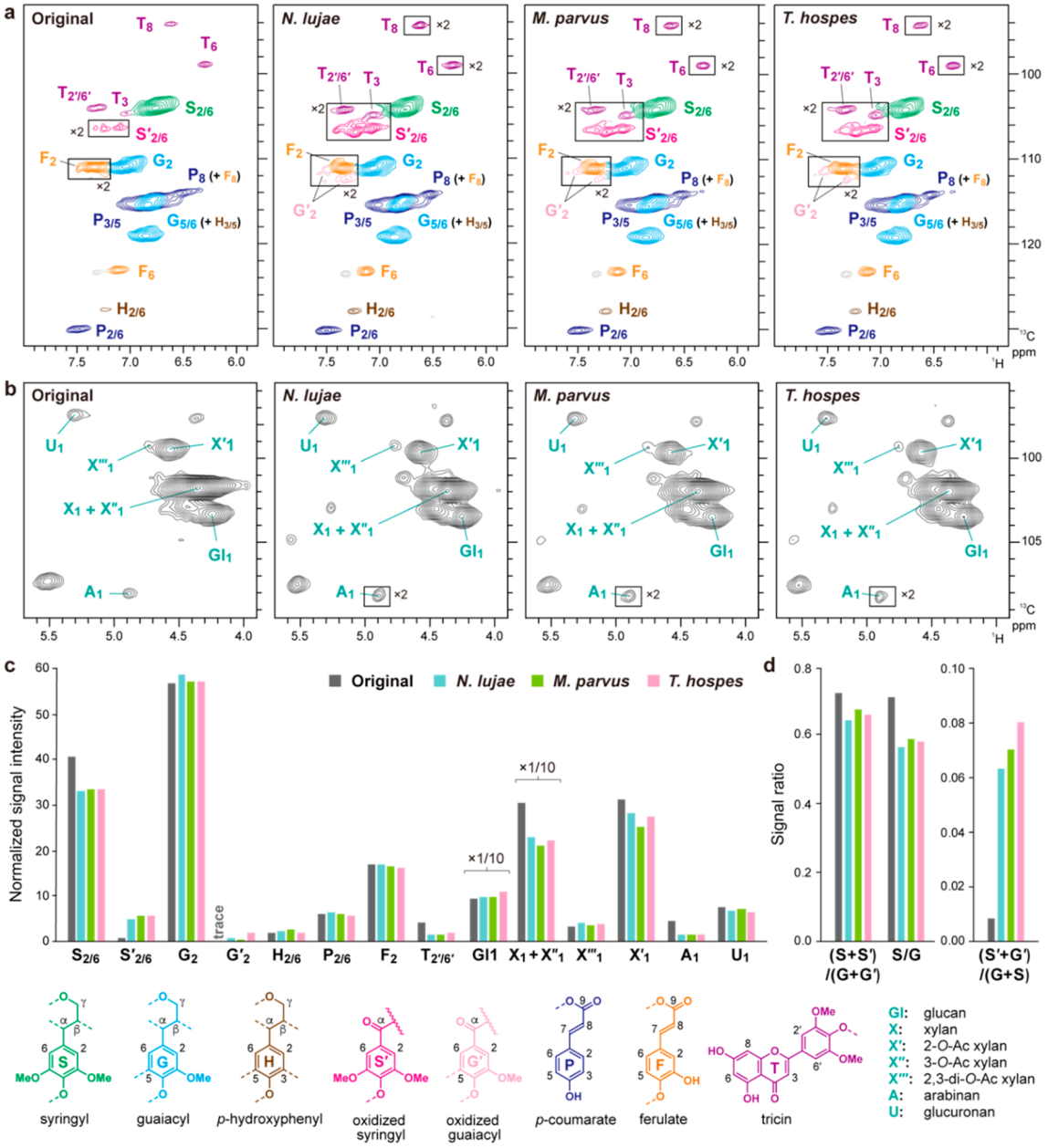

Figure 2. Partial short-range $^{1}H-^{13}C$ correlation (HSQC) NMR spectra of wheat straw cell walls before (original) and after digestion by gut microbiomes from *N. lujae*, *M. parvus*, and *T. hospes*. Aromatic (a) and polysaccharide anomeric (b) subregions are shown. Signal assignments are listed in Table S1. Boxes labeled ×2 represent regions with the scale vertically enlarged by 2-fold. Normalized signal intensity values of major aromatic and anomeric signals expressed on a 1/2S2/6 + 1/2S′2/6 + G2 + G′2 + 1/2H′2/6 = 100 basis (c), and ratios of S (1/2S2/6 and 1/2S′2/6) and G (G2 and *G*′2) aromatic signals (d) are shown. Data labeled ×1/10 indicate that the reported values are divided by a factor 10 for visualization purposes.

GAX may be more tolerant to the microbial digestion compared to the nonacetylated and monoacetylated xylan moieties constituting the main GAX polymer chain. It is noteworthy that the proportion of glucuronan (U) signals was not significantly affected in all the digested samples. This result contradicts the notable reduction of uronic acid contents in the digested cell walls as determined by the wet-chemical analysis (Tables 2 and 3).

In line with the altered S/G lignin unit ratio determined by thioacidolysis, which does not include oxidized forms (S′ and G′) (Table 3), and also partially by py-GC-MS as described below, the ratio of total S and G lignin aromatic units based on the (S + S′)/(G + G′) NMR signal ratio as well as the ratio of nonoxidized S and G units based on the S/G signal ratio decreased in all the digested wheat straw samples (Figure 2c). Intriguingly, we detected considerable augmentations of the C*α*-oxidized S (S′) signals in the digested wheat straw cell wall spectra compared to those in the undigested control cell wall spectrum. The C*α*-oxidized G signals (G′) also apparently increased but in lesser extent to oxidized S signals (S′) (Figure 2c). Consequently, the (S′ + G′)/(S + G) signal ratio remarkably increased in all digested samples, rising up to ca. 10-fold in the spectrum of the cell wall sample digested by the *T. hospes* gut microbiome (Figure 2c). In addition, the lignin-bound tricin signal (T) appeared to be sharply depleted in all the digested cell wall spectra (Figure 2c), suggesting a

https://dx.doi.org/10.1021/acssuschemeng.0c07817
ACS Sustainable Chem. Eng. 2021, 9, 2191−2202

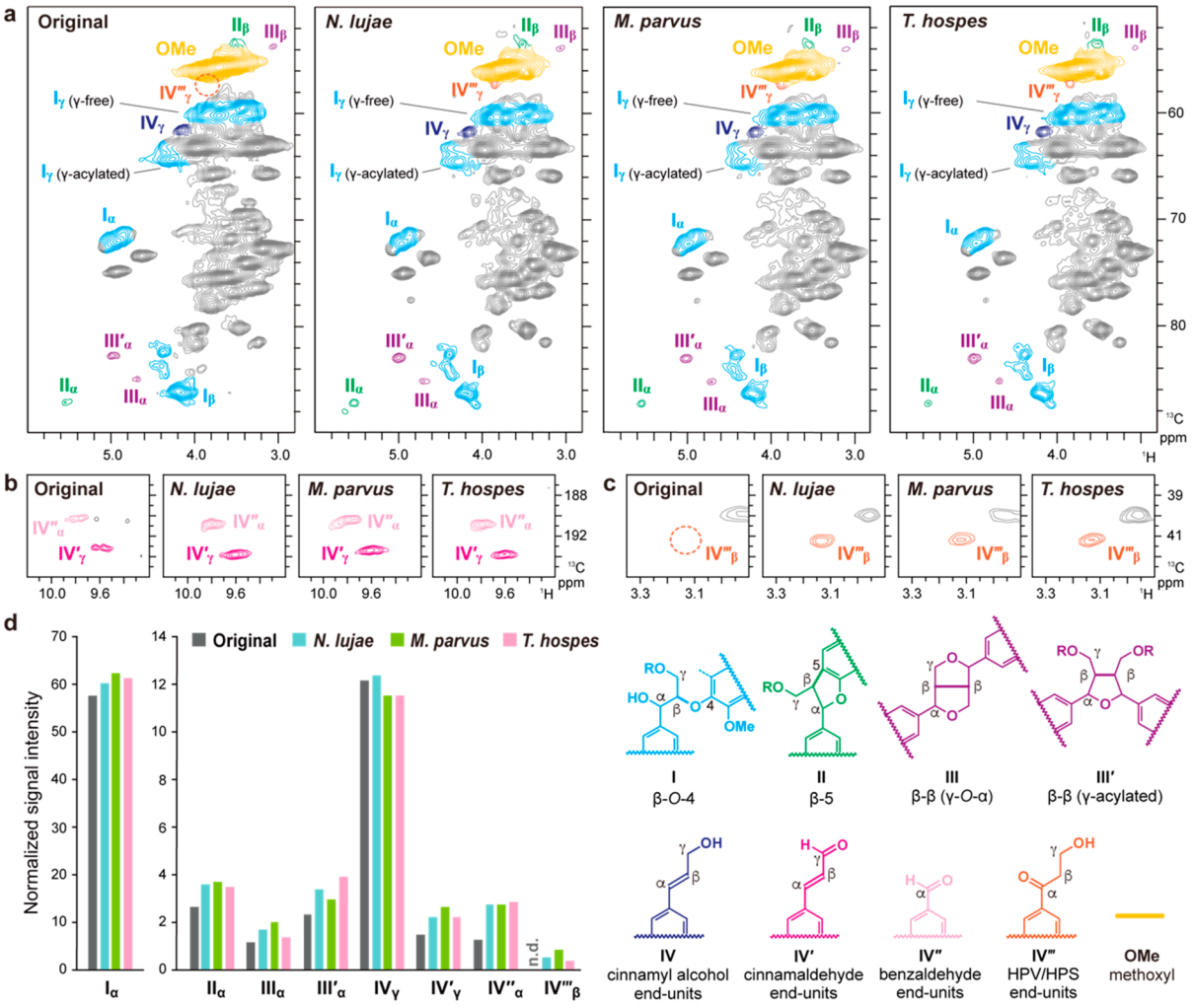

Figure 3. Partial short-range $^{1}H-^{13}C$ correlation (HSQC) NMR spectra of wheat straw cell walls before (original) and after digestion by gut microbiomes from *N. lujae*, *M. parvus*, and *T. hospes*. Oxygenated aliphatic (a, c) and aldehyde (b) subregions are shown. Signal assignments are listed in Table S1. (d) Normalized signal intensity values expressed on a 1/2S2/6 + 1/2S′2/6 + G2 + G′2 + 1/2H′2/6 = 100 basis (see Figure 2) are shown. n.d., not detected.

preferential degradation of lignin-bound tricin units by the termite gut microbes.

We also performed volume integration analysis for the signals from the intermonomeric linkages and end-units in lignin polymer appearing in the oxygenated aliphatic and aldehyde subregions of the HSQC spectra (Figure 3). Overall, no drastic differences in the relative distributions of the major intermonomeric linkage signals, such as those from $\beta-O-4$ (I), $\beta-5$ (II), and $\beta-\beta$ (III and III′) linkages, were detected between the spectra of wheat cell walls before and after digestion by either of the three termite gut microbiomes tested, although in absolute terms (per 100 aromatic rings), augmentations in these intact lignin intermonomeric unit linkages could be observed. The intensities of I, II, III, and III′ signals normalized based on S + S′ + G + G′ + H generally increased in all the digested cell wall spectra compared to the undigested control spectrum (Figure 3d). Meanwhile, we detected increased aldehyde signals from cinnamaldehyde (IV′) and benzaldehyde (IV″) end-units in all the digested wheat straw samples (Figure 3c).

More strikingly, a set of new signals attributed hydroxypropiovanilone (HPV) and hydroxypropiosyringone (HPS) end-units (IV‴; $\delta C/\delta H$, $C\beta-H\beta$ at 41.5/3.14, and $C\gamma-H\gamma$ at 57.0/3.85)[36] appeared clearly in all the digested cell wall spectra, whereas these HPV/HPS (IV‴) signals are undetectable in the undigested cell wall spectra (Figure 3a, c, d). These data are in line with the augmented $C\alpha$-oxidized lignin aromatic unit signals (S′ and G′) in the aromatic subregions (Figure 2c) and further consolidate our notion that lignin polymers are at least partially deconstructed by the action of termite gut microbiomes.

^{13}C-IS py-GC-MS Analysis. Besides quantification of lignin content, ^{13}C-IS py-GC-MS analysis also provides valuable information on lignin structures. The different lignin-derived pyrolysis products of the original and digested wheat straw were classified according to their structural moieties and summarized (Table 4 and Table S2).

The original wheat straw displayed a typical structural composition of grass lignin with a H:G:S ratio of 10:59:30, in agreement with the composition reported in previous studies.[24,25] In addition, 4-vinylphenol and 4-vinylguaiacol, majorly derived from *p*-coumaric acid and ferulic acid, respectively, were present in expected levels, as were the other detailed structural features (Table 4).

^{13}C-IS py-GC-MS analysis of the wheat straw digested by termite gut microbiomes showed a similar subunit composition

https://dx.doi.org/10.1021/acssuschemeng.0c07817
ACS Sustainable Chem. Eng. 2021, 9, 2191−2202

Table 4. ^{13}C-IS py-GC-MS Relative Abundance of Residual Lignin Compounds of Wheat Straw before and after the Digestion by the Gut Microbiomes of *N. lujae*, *M. parvus*, and *T. hospes*[a]

		digested wheat straw		
		gut microbe origin		
	undigested original wheat straw	*N. lujae*	*M. parvus*	*T. hospes*
	Lignin Units (Abundance in mol %)			
H	10.7 ± 1.1	8.5 ± 0.4*	8.8 ± 0.2*	9.1 ± 0.3
G	58.9 ± 1.1	60.9 ± 0.3*	61.9 ± 0.9*	61.9 ± 0.7*
S	30.4 ± 1.0	30.6 ± 0.7	29.4 ± 0.8	29.0 ± 0.9
S/G	0.52 ± 0.02	0.50 ± 0.01	0.48 ± 0.02	0.47 ± 0.02*
	Structural Moieties (Abundance in mol %)			
unsubstituted	5.2 ± 0.14	6.0 ± 0.53	6.4 ± 0.15*	6.2 ± 1.0
methyl	3.23 ± 0.17	3.28 ± 0.19	3.28 ± 0.27	3.69 ± 0.39
vinyl	41.48 ± 1.91	36.19 ± 0.52*	36.14 ± 0.79*	36.17 ± 1.80*
4-VP	9.07 ± 0.96	6.96 ± 0.31*	7.26 ± 0.18*	7.46 ± 0.35*
4-VG	28.31 ± 1.16	25.29 ± 0.38*	25.04 ± 0.95	24.95 ± 1.23
C_α-ox	3.89 ± 0.06	4.06 ± 0.15	3.82 ± 0.09	4.03 ± 0.43
C_β-ox	2.08 ± 0.03	2.14 ± 0.06	2.04 ± 0.11	2.14 ± 0.05
C_γ-ox	40.3 ± 1.96	44.3 ± 0.35*	44.5 ± 1.36*	43.5 ± 1.84
miscellaneous	3.84 ± 0.13	4.02 ± 0.14	3.86 ± 0.22	4.26 ± 0.19
PhC3	45.31 ± 2.01	49.59 ± 0.44*	49.58 ± 1.20*	49.06 ± 1.97

[a]Values are expressed as means ± SD. Statistical differences are marked with * ($p < 0.05$, $n = 3$, Student's *t*-test); 4-VP = 4-vinylphenol; 4-VG = 4-vinylguaiacol; PhC3 = phenols with intact α, β, and γ carbon side-chain, excluding diketones.

as the undigested wheat straw, with minimal variation between the species (H:G:S *N. lujae* 8:61:31, *M. parvus* 8:62:30, *T. hospes* 9:62:29). Compared to undigested wheat straw, a slight decrease in S/G ratio was observed, particularly for *T. hospes*. These observations are consistent with the aromatic compositional analyses based on thioacidolysis (Table 3) and 2D HSQC NMR (Figure 2).

Even though the overall subunit composition did not differ between undigested and digested wheat straw, a more detailed structural classification revealed significant differences (Table 4), but with little variation between the termite species. A significant decrease of vinyl products (~13%) was observed in digested straws, which was primarily due to decreases in 4-vinylphenol (~20%) and 4-vinylguaiacol (~12%). This suggests the targeted removal of the corresponding hydroxycinnamic acids *p*CA and FA, which these products are largely, yet not exclusively, derived of, again in line with the slight decrease of these moieties as observed by NMR analysis (Figure 2c).

Interestingly, Cγ-oxidized pyrolysis products were found to be significantly increased (~10%) upon digestion, concomitantly also increasing the abundance of pyrolysis products with an intact α,β,γ side-chain (PhCγ) to similar extents. We have previously established that these products correlate well with the amount of intact interunit linkages present, as determined by HSQC NMR.[25,40,41] Indeed, also the NMR analysis showed a relative increase of intact interunit linkages (per 100 aromatic rings) (Figure 3d).

Despite the fact that the NMR analyses showed a significant augmentation of benzaldehyde units in the digested samples (Figure 3b, d), neither the grouped Cα-oxidized pyrolysis products (Table 4) nor vanillin and syringaldehyde (Table S2) displayed significant differences in comparison to the undigested wheat straw sample. However, their respective decarbonylated analogues, guaiacol and syringol, did increase (Table S2). Aldehyde decarbonylation reactions are likely to occur during pyrolysis, but note that guaiacol and syringol are formed from a wealth of other substructures and, therefore, should not be interpreted as markers for the occurrence of benzaldehyde substructures. Interestingly, coinciding with the increase of Cα-oxidized subunits, the HPV/HPS end-units became apparent in the NMR spectra of the treated samples (Figure 3). We have previously shown that these structures give rise to acetovanillone/guaiacyl vinyl ketone and acetosyringone/syringyl vinyl ketone upon pyrolysis, respectively.[40] Indeed, our py-GC-MS analysis here showed that the former marker products increased approximately 20% in the digested samples (from 0.55% to 0.65% of the relative abundance of lignin-derived pyrolysis products), whereas the latter pair was not significantly different (Table S2). Overall, our data further corroborate the appearance of the HPV/HPS moieties during the digestion with termite gut microbes.

DISCUSSION

To gain insights into the fate of wheat straw lignin after digestion by gut microbiomes of higher termites in anaerobic bioreactors, we combined wet chemistry, 2D HSQC NMR, and ^{13}C-IS py-GC-MS measurements. Collectively, our findings suggest that lignin polymer in wheat straw is partially modified and/or depolymerized by the gut microbiomes when implemented in anaerobic bioreactors. Nevertheless, in line with previous observations,[20,22,23] all the termite gut microbiomes tested in this study preferentially used polysaccharides, rather than lignin, as preferential carbon sources (Tables 2 and 3). In particular, the changes in GAX fractions as assessed by wet chemistry (Tables 2 and 3) and 2D HSQC NMR (Figure 2) suggested that they are more susceptible toward microbial degradation than cellulose and lignin. Consequently, the lignocellulose composition of the digested wheat straw residues presented largely increased lignin contents (by ca. 23 ± 10%) compared with the undigested wheat straw (Table 2). Previous studies reported similar results, showing lignin accumulation in termite faeces, suggesting no degradation of lignin by termites.[42] Importantly, however, our estimation of absolute lignocellulose compositional changes considering the VS loss

https://dx.doi.org/10.1021/acssuschemeng.0c07817
ACS Sustainable Chem. Eng. 2021, 9, 2191−2202

(Table 1) suggested that a considerable portion of lignin (26 ± 10%) was also removed along with polysaccharides during the microbial degradation (Figure 1), suggesting that the termite gut microbiomes indeed harbor an ability to remove wheat straw lignin in anaerobic bioreactors. We like to point out that, based on our structural analyses by 2D HSQC NMR and py-GC-MS, it is estimated that at least 80% of the observed delignification can be attributed to the true removal of lignin, rather than the removal of *p*-coumaric acid, ferulic acid, and tricin moieties.

Our thioacidolysis, 2D HSQC NMR, and py-GC-MS analyses provided overall consistent lignin compositional changes induced by the termite gut microbiomes. While the total S and G lignin unit analysis by py-GC-MS and 2D HSQC NMR (based on the signal ratio of the sums of non-Cα-oxidized and Cα-oxidized S + S′ and G + G′) suggested overall little changes in the total S/G lignin unit ratio (Figure 2 and Table 4), the ratio of the nonoxidized S/G lignin units as estimated by thioacidolysis (based on the β−O−4-derived S/G monomer ratio), and 2D HSQC NMR (based on the signal ratio of only non-Cα-oxidized S and G) appeared to be decreased in all the digested cell wall samples (Table 3 and Figure 2). Collectively, these data suggested that S units in the original wheat lignin polymer might be more preferentially modified than G units and, most likely, converted into the corresponding Cα-oxidized S units by the gut microbiomes of higher termites in the anaerobic bioreactors, which will be elaborated on below. 2D HSQC NMR also showed a high level of tricin depletion (ca. 50−65% reductions) in lignin residues left after the digestion. The preferential degradation of tricin or tricin-containing fractions by termites is interesting given the fact that these moieties were shown to (relatively) accumulate in biological oxidative delignification strategies, both by the white-rot fungi *Ceriporiopsis subvermispora* and laccase-mediator treatments.[39] Nevertheless, it has also been shown that tricin can be removed by either chemical[43] or biological processes,[25] probably due to its terminal position in the polymeric chain of grass lignin.[37] For instance, previous studies focused on lignin degradation by *Pleurotus eryngii* showed a strong removal of tricin. Similarly, a preferential removal of oligomeric lignin fractions containing tricin terminal units was observed in the degradation of rice lignocellulose in the *C. formosanus* gut digestive system.[20]

The evidence for lignin side-chain modifications induced by the termite gut microbes was obtained by both 2D HSQC NMR and py-GC-MS. Most strikingly, they both clearly detected, albeit at low levels, the appearance of the HPV/HPS end-units harboring Cα-oxidized side-chains in the digested lignin residues (Figure 3, Table 4, and Table S2). Side-chain oxidation of Cα is characteristic of lignin modification induced by white-rot fungi,[44] and it has also been previously observed in feces of the beetle *Anoplophora glabripennis* and the lower termite *Zootermopsis angusticollis* that digest wood anaerobically.[45] In the present work, the increase of Cα-oxidized aromatic signals is partially associated with the increases in HPV/HPS end-units (Figure 2, Table 4, and Table S2). The HPV/HPS products have been described for lignin degradation by the action of β-etherases, enzymes that degrade lignin in a reductive cascade.[46] The presence of β-etherases, particularly of glutathione-dependent-β-etherases cleaving β-aryl-ether lignin compounds, was first reported in *Sphingobium* sp.[47,48] Since then, its activity on polymeric lignin has been demonstrated,[48,49] and its presence has also been reported in multiple bacteria including anaerobic strains such as *Tolumonas lignolytica*.[50] Most of the bacterial species harboring homologous glutathione-dependent β-etherase genes fall into the Proteobacteria phylum, members of which have been also found in termite guts.[51,52] The gut of termites hosts a large variety of microbes, and in the termite species studied here, Proteobacteria represented up to 11% of the total gut microbiome. This fraction increased during the bioreactor experiments reaching up to 40% of the total community.[26] Overall, our results could suggest that bacteria harboring β-etherase genes may have been involved in the cleavage of β−O−4 linkages in the lignin polymer in the current bioreactor experiments. β-Etherases are thus far thought to be enzymes associated with the cell membrane,[48] and their activity on polymeric lignin has only be demonstrated in *in vitro* experiments.[48,49] Nevertheless, although there is no experimental evidence for this hypothesis, β-etherases could still be transported extracellularly in dedicated outer membrane vesicles, as it has been observed for enzymes acting on lignin-derived aromatics, and upon lysis of these vesicles act on polymeric lignin.[53] To our knowledge, no earlier study on lignocellulose deconstruction by termite gut microbiomes has observed the appearance of HPV/HPS in degraded lignin residues, providing potential evidence of the involvement of lignin β-etherases in the termite gut microbiome.

In addition to the HPV/HPS signatures, 2D HSQC NMR also detected considerably augmented aldehyde end-units, which, unlike HPV/HPS, might be the result of cleavage of the Cα−Cβ bond[51] in the digested lignin residues (Figure 3). Previous py-GC-MS-aided structural studies on lignin degradation by several lower termite species reported pyrograms displaying phenolic compounds annotated as markers for oxidized lignin side-chains.[17,23,45] Meanwhile, however, a recent study employing 2D HSQC NMR for dissecting lignin degradation by a lower termite *C. formosanus* detected no clear evidence for such lignin side-chain oxidation.[20] Although the appearance of the aldehyde end-units in lignin has been described as typical consequences of oxidative lignin degradation undertaken by wood-decaying fungi harboring strong lignin oxidases,[54] it is fairly doubtful that similar lignin oxidation cascades can be operative during lignin degradation by the termite gut microbiomes under strictly anaerobic conditions. Even though bacterial strains with lignin peroxidase activity have been isolated from termite digestive systems,[55,56] and members of the *Pseudomonas* genus producing an elaborate lignin-active enzymatic arsenal,[57] their involvement during anaerobic lignin degradation remains elusive. Interestingly, putative peroxidase genes, including glutathione and DyP-type peroxidases, and multiple cytochrome oxidases were found in anaerobic lignin-degrading Enterobacteriaceae (γ-Protobacteria),[58,59] members of which were found in our bioreactors, and hence could have been involved.[26] Clearly, future studies should further explore this aspect in combination with advanced meta-omics analysis to reveal new lignin degradation pathways, enzymes, and microorganisms responsible for the appearance of such oxidized lignin structures, in particular under anaerobic conditions.

Since both 2D HSQC NMR and py-GC-MS suggested overall increases of intact lignin intermonomeric linkages per total lignin aromatic units in the digested lignin residues (Figure 3 and Table 4), major lignin degradation pathways operated by the termite gut microbiomes may involve cleavages of C−C-bonded (condensed) lignin substructures

https://dx.doi.org/10.1021/acssuschemeng.0c07817
ACS Sustainable Chem. Eng. 2021, 9, 2191−2202

which cannot in general be well assessed by the current NMR and py-GC-MS analyses. Likewise, previous NMR studies on lignin degradations by a lower termite *C. formosanus*[20] and fungus-cultivating higher termite *Odontotermes formosanus*[21] noted similar views based on their observations of proportionally increased intact β−O−4 linkages in the digested lignin residues. Given the limited degree of structural modifications in the digested lignin residues as assessed by NMR and py-GC-MS, the net removal of lignin measured in the current bioreactor experiments, estimated as to be up to ca. 37% (Figure 2), was rather remarkable. As proposed in previous studies,[23] the preferential degradation of hemicelluloses by gut microbiomes might facilitate the removal of lignin fractions cross-linked to hemicelluloses. Indeed, it is well-known that a significant portion of grass lignin is covalently cross-linked to GAX via ferulates; the microbial production of feruloyl esterases has been previously observed in metatranscriptomic studies of the termite microbiome[60] and could provide the means to decouple them.[6,7] More in-depth structural analyses of degraded lignin fractions including those potentially present in the liquid fractions of the bioreactors are required to clarify these aspects. Such lignin structural studies, in combination with metagenomic, metatranscriptomic, metaproteomic, and biochemical characterizations of termite gut microbiomes, would provide further insights into the elusive mechanisms of lignocellulose biodegradation by wood-feeding insects and contribute to their potential applications for lignocellulose biorefineries.

■ ASSOCIATED CONTENT

Supporting Information

The Supporting Information is available free of charge at https://pubs.acs.org/doi/10.1021/acssuschemeng.0c07817.

Peak assignments for 2D HSQC NMR spectra; identity, structural classification, and relative abundance of lignin-derived pyrolysis products by quantitative ^{13}C-IS py-GC-MS; average relative abundance of analytical triplicates; methods; and a detailed description of the experimental methodology (PDF)

■ AUTHOR INFORMATION

Corresponding Author

Guillermina Hernandez-Raquet − *Toulouse Biotechnology Institute, TBI, Université de Toulouse, CNRS, INRAE, INSA, 31077 Toulouse, France;* orcid.org/0000-0003-4465-4607; Phone: +33 5 61 55 99 77; Email: hernandg@insa-toulouse.fr

Authors

Louison Dumond − *Toulouse Biotechnology Institute, TBI, Université de Toulouse, CNRS, INRAE, INSA, 31077 Toulouse, France*

Pui Ying Lam − *Research Institute for Sustainable Humanosphere, Kyoto University, Uji, Kyoto 611-0011, Japan*

Gijs van Erven − *Laboratory of Food Chemistry, Wageningen University & Research, 6708 WG Wageningen, The Netherlands; Wageningen Food & Biobased Research, 6708 WG Wageningen, The Netherlands*

Mirjam Kabel − *Laboratory of Food Chemistry, Wageningen University & Research, 6708 WG Wageningen, The Netherlands;* orcid.org/0000-0002-1544-1744

Fabien Mounet − *Laboratoire de Recherche en Sciences Végétales, Université de Toulouse III, CNRS, UPS, UMR 5546, 31320 Castanet-Tolosan, France*

Jacqueline Grima-Pettenati − *Laboratoire de Recherche en Sciences Végétales, Université de Toulouse III, CNRS, UPS, UMR 5546, 31320 Castanet-Tolosan, France*

Yuki Tobimatsu − *Research Institute for Sustainable Humanosphere, Kyoto University, Uji, Kyoto 611-0011, Japan;* orcid.org/0000-0002-7578-7392

Complete contact information is available at: https://pubs.acs.org/10.1021/acssuschemeng.0c07817

Author Contributions

L.D. prepared the samples and carried out and analyzed wet-chemistry experiments with thioacidolysis performed under F.M.'s supervision. P.Y.L. and Y.T. carried out and analyzed 2D HSQC NMR experiments. G.v.E. and M.K. performed and analyzed py-GC-MS experiments. As project coordinator, G.H.-R. designed the study, participated in experimental design, and contributed at all stages. The manuscript was written by L.D. under G.H.-R.'s supervision and with important intellectual contributions from all authors. All authors have given approval to the final version of the manuscript. G.H.-R. and Y.T. participated in funding this research.

Notes

The authors declare no competing financial interest.

■ ACKNOWLEDGMENTS

The authors thank Dr. Hironori Kaji and Ms. Ayaka Maeno (ICR, Kyoto University) for their support in NMR experiments. This study was supported in part by PHC Sakura Program from MAEDI-MENESR and the Japan Society for the Promotion of Science (JSPS), JSPS KAKENHI grants (grant JP#16H06198 and JP#20H03044), and a research grant from Exploratory Research on Sustainable Humanosphere Science from RISH, Kyoto University. A part of this study was conducted using the facilities in the DASH/FBAS of RISH, Kyoto University, and the NMR spectrometer at the JURC of ICR, Kyoto University. This work has received funding from the Bio Based Industry Joint Undertaking under the European Union's Horizon 2020 research and innovation program under grant 720303 (EU-Zelcor, Zero waste lignocellulosic biorefineries by integrated lignin valorization). It was also supported by the French National Institute of Research for Agriculture, Food and Environment (INRAE), the Region Languedoc-Roussillon Midi-Pyrénées grant 31000553, the Carnot Institute 3BCAR−Insyme project and the PHC Sakura program from Campus France under the project 45094PM. The authors thank the GeT Plage platform of INRAE Toulouse, E. Mengelle, M. Bounouba, and S. Dubos for the technical support with bioreactor experiments.

■ REFERENCES

(1) European Union. Directive (EU) 2015/1513 of the european parliament and of the council of 9 september 2015 amending directive 98/70/EC relating to the quality of petrol and diesel fuels and amending Directive 2009/28/EC on the promotion of the use of energy from renewable sources (text with EEA relevance); 15.9.2015. *OJ. L* **2015**, *239*, 1−29.

(2) Lapierre, C.; Pollet, B.; Rolando, C. New insights into the molecular architecture of hardwood lignins by chemical degradative methods. *Res. Chem. Intermed.* **1995**, *21*, 397−412.

(3) del Río, J. C.; Rencoret, J.; Prinsen, P.; Martínez, Á. T.; Ralph, J.; Gutiérrez, A. Structural characterization of wheat straw lignin as revealed by analytical pyrolysis, 2D-NMR, and reductive cleavage methods. *J. Agric. Food Chem.* **2012**, *60*, 5922−5935.
(4) Liu, Q.; Luo, L.; Zheng, L. Lignins: biosynthesis and biological functions in plants. *Int. J. Mol. Sci.* **2018**, *19* (2), 335.
(5) Kamimura, N.; Sakamoto, S.; Mitsuda, N.; Masai, E.; Kajita, S. Advances in microbial lignin degradation and its applications. *Curr. Opin. Biotechnol.* **2019**, *56*, 179−186.
(6) Ralph, J.; Lapierre, C.; Boerjan, W. Lignin structure and its engineering. *Curr. Opin. Biotechnol.* **2019**, *56*, 240−249.
(7) Karlen, S. D.; Zhang, C.; Peck, M. L.; Smith, R. A.; Padmakshan, D.; Helmich, K. E.; Free, H. C. A.; Lee, S.; Smith, B. G.; Lu, F.; Sedbrook, J. C.; Sibout, R.; Grabber, J. H.; Runge, T. M.; Mysore, K. S.; Harris, P. J.; Bartley, L. E.; Ralph, J. Monolignol ferulate conjugates are naturally incorporated into plant lignins. *Sci. Adv.* **2016**, *2*, e1600393.
(8) Sigoillot, J.-C.; Berrin, J.-G.; Bey, M.; Lesage-Meessen, L.; Levasseur, A.; Lomascolo, A.; Record, E.; Uzan-Boukhris, E. Chapter 8 - Fungal strategies for lignin degradation. In *Advances in Botanical Research*; Jouanin, L., Lapierre, C., Eds.; Lignins; Academic Press, 2012; Vol. *61*, pp 263−308. DOI: 10.1016/B978-0-12-416023-1.00008-2.
(9) Masai, E.; Katayama, Y.; Fukuda, M. Genetic and biochemical investigations on bacterial catabolic pathways for lignin-derived aromatic compounds. *Biosci., Biotechnol., Biochem.* **2007**, *71*, 1−15.
(10) Lambertz, C.; Garvey, M.; Klinger, J.; Heesel, D.; Klose, H.; Fischer, R.; Commandeur, U. Challenges and advances in the heterologous expression of cellulolytic enzymes: a review. *Biotechnol. Biofuels* **2014**, *7* (135), 1−15.
(11) Crawford, D. L.; Crawford, R. L. Microbial degradation of lignin. *Enzyme Microb. Technol.* **1980**, *2*, 11−22.
(12) Zeng, J.; Singh, D.; Laskar, D. D.; Chen, S. Degradation of native wheat straw lignin by *Streptomyces viridosporus* T7A. *Int. J. Environ. Sci. Technol.* **2013**, *10*, 165−174.
(13) Riyadi, F. A.; Tahir, A. A.; Yusof, N.; Sabri, N. S. A.; Noor, M. J. M. M.; Akhir, F. N. M. D.; Othman, N.; Zakaria, Z.; Hara, H. Enzymatic and genetic characterization of lignin depolymerization by *Streptomyces sp.* S6 isolated from a tropical environment. *Sci. Rep.* **2020**, *10* (7813), 1−9.
(14) Salvachúa, D.; Karp, E. M.; Nimlos, C. T.; Vardon, D. R.; Beckham, G. T. Towards lignin consolidated bioprocessing: simultaneous lignin depolymerization and product generation by bacteria. *Green Chem.* **2015**, *17*, 4951−4967.
(15) Brune, A. Symbiotic digestion of lignocellulose in termite guts. *Nat. Rev. Microbiol.* **2014**, *12*, 168−180.
(16) Kato, K.; Kozaki, S.; Sakuranaga, M. Degradation of lignin compounds by bacteria from termite guts. *Biotechnol. Lett.* **1998**, *20*, 459−462.
(17) Ke, J.; Singh, D.; Chen, S. Aromatic compound degradation by the wood-feeding termite Coptotermes formosanus (Shiraki). *Int. Biodeterior. Biodegrad.* **2011**, *65*, 744−756.
(18) Kim, H.; Ralph, J. Solution-state 2D NMR of ball-milled plant cell wall gels in DMSO-D6/Pyridine-D5. Org. *Org. Biomol. Chem.* **2010**, *8*, 576−591.
(19) Mansfield, S. D.; Kim, H.; Lu, F.; Ralph, J. Whole plant cell wall characterization using solution-state 2D NMR. *Nat. Protoc.* **2012**, *7*, 1579−1589.
(20) Tarmadi, D.; Tobimatsu, Y.; Yamamura, M.; Miyamoto, T.; Miyagawa, Y.; Umezawa, T.; Yoshimura, T. NMR studies on lignocellulose deconstructions in the digestive system of the lower termite *Coptotermes formosanus* Shiraki. *Sci. Rep.* **2018**, *8* (1290), 1−9.
(21) Li, H.; Yelle, D. J.; Li, C.; Yang, M.; Ke, J.; Zhang, R.; Liu, Y.; Zhu, N.; Liang, S.; Mo, X.; Ralph, J.; Currie, C. R.; Mo, J. Lignocellulose pretreatment in a fungus-cultivating termite. *Proc. Natl. Acad. Sci. U. S. A.* **2017**, *114*, 4709−4714.
(22) Katsumata, K. S.; Jin, Z.; Hori, K.; Iiyama, K. Structural changes in lignin of tropical woods during digestion by termite, *Cryptotermes brevis*. *J. Wood Sci.* **2007**, *53*, 419−426.
(23) Ke, J.; Laskar, D. D.; Chen, S. Varied lignin disruption mechanisms for different biomass substrates in lower termite. *Renewable Energy* **2013**, *50*, 1060−1064.
(24) van Erven, G.; de Visser, R.; Merkx, D. W. H.; Strolenberg, W.; de Gijsel, P.; Gruppen, H.; Kabel, M. A. Quantification of lignin and its structural features in plant biomass using 13C lignin as internal standard for pyrolysis-GC-SIM-MS. *Anal. Chem.* **2017**, *89*, 10907−10916.
(25) van Erven, G.; Nayan, N.; Sonnenberg, A. S. M.; Hendriks, W. H.; Cone, J. W.; Kabel, M. A. Mechanistic insight in the selective delignification of wheat straw by three white-rot fungal species through quantitative 13C-IS Py-GC-MS and whole cell wall HSQC NMR. *Biotechnol. Biofuels* **2018**, *11* (262), 1−16.
(26) Auer, L.; Lazuka, A.; Sillam-Dussès, D.; Miambi, E.; O'Donohue, M.; Hernandez-Raquet, G. Uncovering the potential of termite gut microbiome for lignocellulose bioconversion in anaerobic batch bioreactors. *Front. Microbiol.* **2017**, *8* (2623), 1−14.
(27) Cavaillé, L.; Grousseau, E.; Pocquet, M.; Lepeuple, A.-S.; Uribelarrea, J.-L.; Hernandez-Raquet, G.; Paul, E. Polyhydroxybutyrate production by direct use of waste activated sludge in phosphorus-limited fed-batch culture. *Bioresour. Technol.* **2013**, *149*, 301−309.
(28) Lazuka, A.; Auer, L.; Bozonnet, S.; Morgavi, D. P.; O'Donohue, M.; Hernandez-Raquet, G. Efficient anaerobic transformation of raw wheat straw by a robust cow rumen-derived microbial consortium. *Bioresour. Technol.* **2015**, *196*, 241−249.
(29) Méchin, V.; Laluc, A.; Legée, F.; Cézard, L.; Denoue, D.; Barrière, Y.; Lapierre, C. Impact of the Brown-Midrib Bm5 mutation on maize lignins. *J. Agric. Food Chem.* **2014**, *62*, 5102−5107.
(30) Ployet, R. *Régulation de la formation du bois chez l'eucalyptus lors du développement et en réponse a des contraintes environnementales*. PhD, Université de Toulouse, Université Toulouse III—Paul Sabatier, 2017.
(31) Tobimatsu, Y.; Chen, F.; Nakashima, J.; Escamilla-Treviño, L. L.; Jackson, L.; Dixon, R. A.; Ralph, J. Coexistence but independent biosynthesis of catechyl and guaiacyl/syringyl lignin polymers in seed coats. *Plant Cell* **2013**, *25*, 2587−2600.
(32) Lam, P. Y.; Tobimatsu, Y.; Takeda, Y.; Suzuki, S.; Yamamura, M.; Umezawa, T.; Lo, C. Disrupting flavone synthase ii alters lignin and improves biomass digestibility. *Plant Physiol.* **2017**, *174*, 972−985.
(33) van Erven, G.; de Visser, R.; de Waard, P.; van Berkel, W. J. H.; Kabel, M. A. Uniformly ^{13}C labeled lignin internal standards for quantitative pyrolysis-GC-MS analysis of grass and wood. *ACS Sustainable Chem. Eng.* **2019**, *7*, 20070−20076.
(34) Lapierre, C.; Monties, B.; Rolando, C.; Chirale, L. de. Thioacidolysis of lignin: comparison with acidolysis. *J. Wood Chem. Technol.* **1985**, *5*, 277−292.
(35) Rolando, C.; Monties, B.; Lapierre, C. Thioacidolysis. In *Methods in lignin chemistry; Springer Series in Wood Science*; Springer: Berlin, Heidelberg, 1992; pp 334−349. DOI: 10.1007/978-3-642-74065-7_23.
(36) Karlen, S. D.; Free, H. C. A.; Padmakshan, D.; Smith, B. G.; Ralph, J.; Harris, P. J. Commelinid monocotyledon lignins are acylated by p-coumarate. *Plant Physiol.* **2018**, *177*, 513−521.
(37) Lan, W.; Lu, F.; Regner, M.; Zhu, Y.; Rencoret, J.; Ralph, S. A.; Zakai, U. I.; Morreel, K.; Boerjan, W.; Ralph, J. Tricin, a flavonoid monomer in monocot lignification. *Plant Physiol.* **2015**, *167*, 1284−1295.
(38) Lam, P. Y.; Tobimatsu, Y.; Matsumoto, N.; Suzuki, S.; Lan, W.; Takeda, Y.; Yamamura, M.; Sakamoto, M.; Ralph, J.; Lo, C.; Umezawa, T. OsCAldOMT1 Is a bifunctional O -methyltransferase involved in the biosynthesis of tricin-lignins in rice cell walls. *Sci. Rep.* **2019**, *9*, 1−13.
(39) Martin, A. F.; Tobimatsu, Y.; Kusumi, R.; Matsumoto, N.; Miyamoto, T.; Lam, P. Y.; Yamamura, M.; Koshiba, T.; Sakamoto, M.; Umezawa, T. Altered lignocellulose chemical structure and molecular assembly in cinnamyl alcohol dehydrogenase-deficient rice. *Sci. Rep.* **2019**, *9* (17153), 1−14.

(40) van Erven, G.; Hilgers, R.; Waard, P. de; Gladbeek, E.-J.; van Berkel, W. J. H.; Kabel, M. A. Elucidation of in situ ligninolysis mechanisms of the selective white-rot fungus *Ceriporiopsis subvermispora*. *ACS Sustainable Chem. Eng.* **2019**, *7*, 16757−16764.
(41) van Erven, G.; Wang, J.; Sun, P.; de Waard, P.; van der Putten, J.; Frissen, G. E.; Gosselink, R. J. A.; Zinovyev, G.; Potthast, A.; van Berkel, W. J. H.; Kabel, M. A. Structural motifs of wheat straw lignin differ in susceptibility to degradation by the white-rot fungus *Ceriporiopsis subvermispora*. *ACS Sustainable Chem. Eng.* **2019**, *7*, 20032−20042.
(42) Cookson, L. J. 14C-Lignin degradation by three Australian termite species. *Wood Sci. Technol.* **1987**, *21*, 11−25.
(43) Miyamoto, T.; Mihashi, A.; Yamamura, M.; Tobimatsu, Y.; Suzuki, S.; Takada, R.; Kobayashi, Y.; Umezawa, T. Comparative analysis of lignin chemical structures of sugarcane bagasse pretreated by alkaline, hydrothermal, and dilute sulfuric acid methods. *Ind. Crops Prod.* **2018**, *121*, 124−131.
(44) van Kuijk, S. J. A.; Sonnenberg, A. S. M.; Baars, J. J. P.; Hendriks, W. H.; del Río, J. C.; Rencoret, J.; Gutiérrez, A.; de Ruijter, N. C. A.; Cone, J. W. Chemical changes and increased degradability of wheat straw and oak wood chips treated with the white rot fungi *Ceriporiopsis subvermispora* and *Lentinula edodes*. *Biomass Bioenergy* **2017**, *105*, 381−391.
(45) Geib, S. M.; Filley, T. R.; Hatcher, P. G.; Hoover, K.; Carlson, J. E.; Jimenez-Gasco, M.; del, M.; Nakagawa-Izumi, A.; Sleighter, R. L.; Tien, M. Lignin degradation in wood-feeding insects. *Proc. Natl. Acad. Sci. U. S. A.* **2008**, *105*, 12932−12937.
(46) Higuchi, Y.; Aoki, S.; Takenami, H.; Kamimura, N.; Takahashi, K.; Hishiyama, S.; Lancefield, C. S.; Ojo, O. S.; Katayama, Y.; Westwood, N. J.; Masai, E. Bacterial catabolism of β-hydroxypropiovanillone and β-hydroxypropiosyringone produced in the reductive cleavage of arylglycerol-β-aryl ether in lignin. *Appl. Environ. Microbiol.* **2018**, *84*, 1−21.
(47) Gall, D. L.; Ralph, J.; Donohue, T. J.; Noguera, D. R. A Group of sequence-related sphingomonad enzymes catalyzes cleavage of β-aryl ether linkages in lignin β-guaiacyl and β-syringyl ether dimers. *Environ. Sci. Technol.* **2014**, *48*, 12454−12463.
(48) Masai, E.; Katayama, Y.; Nishikawa, S.; Yamasaki, M.; Morohoshi, N.; Haraguchi, T. Detection and localization of a new enzyme catalyzing the beta-aryl ether cleavage in the soil bacterium (*Pseudomonas paucimobilis* SYK-6). *FEBS Lett.* **1989**, *249*, 348−352.
(49) Gall, D. L.; Kontur, W. S.; Lan, W.; Kim, H.; Li, Y.; Ralph, J.; Donohue, T. J.; Noguera, D. R. In vitro enzymatic depolymerization of lignin with release of syringyl, guaiacyl, and tricin units. *Appl. Environ. Microbiol.* **2018**, *84*, 1−17.
(50) Billings, A. F.; Fortney, J. L.; Hazen, T. C.; Simmons, B.; Davenport, K. W.; Goodwin, L.; Ivanova, N.; Kyrpides, N. C.; Mavromatis, K.; Woyke, T.; DeAngelis, K. M. Genome sequence and description of the anaerobic lignin-degrading bacterium *Tolumonas lignolytica* sp. nov. *Stand. Genomic Sci.* **2015**, *10* (106), 1−11.
(51) Kontur, W. S.; Olmsted, C. N.; Yusko, L. M.; Niles, A. V.; Walters, K. A.; Beebe, E. T.; Meulen, K. A. V.; Karlen, S. D.; Gall, D. L.; Noguera, D. R.; Donohue, T. J. A Heterodimeric glutathione s-transferase that stereospecifically breaks lignin's β(r)-aryl ether bond reveals the diversity of bacterial β-etherases. *J. Biol. Chem.* **2019**, *294*, 1877−1890.
(52) Voß, H.; Heck, C. A.; Schallmey, M.; Schallmey, A. Database mining for novel bacterial β-etherases, glutathione-dependent lignin-degrading enzymes. *Appl. Environ. Microbiol.* **2020**, *86*, 1−15.
(53) Salvachúa, D.; Werner, A. Z.; Pardo, I.; Michalska, M.; Black, B. A. Outer membrane vesicles catabolize lignin-derived aromatic compounds in *Pseudomonas putida* KT2440. *Proc. Natl. Acad. Sci. U. S. A.* **2020**, *117*, 9302−9310.
(54) Yelle, D. J.; Ralph, J.; Lu, F.; Hammel, K. E. Evidence for cleavage of lignin by a brown rot basidiomycete. *Environ. Microbiol.* **2008**, *10*, 1844−1849.
(55) Zhou, H.; Guo, W.; Xu, B.; Teng, Z.; Tao, D.; Lou, Y.; Gao, Y. Screening and identification of lignin-degrading bacteria in termite gut and the construction of LiP-expressing recombinant *Lactococcus lactis*. *Microb. Pathog.* **2017**, *112*, 63−69.
(56) Le Roes-Hill, M.; Rohland, J.; Burton, S. Actinobacteria isolated from termite guts as a source of novel oxidative enzymes. *Antonie van Leeuwenhoek* **2011**, *100*, 589−605.
(57) Prabhakaran, M.; Couger, M. B.; Jackson, C. A.; Weirick, T.; Fathepure, B. Z. Genome sequences of the lignin-degrading Pseudomonas sp. strain YS-1p and *Rhizobium sp*. strain YS-1r isolated from decaying wood. *Genome Announc.* **2015**, *3*, 1−2.
(58) Woo, H. L.; Ballor, N. R.; Hazen, T. C.; Fortney, J. L.; Simmons, B.; Davenport, K. W.; Goodwin, L.; Ivanova, N.; Kyrpides, N. C.; Mavromatis, K.; Woyke, T.; Jansson, J.; Kimbrel, J.; DeAngelis, K. M. Complete genome sequence of the lignin-degrading bacterium *Klebsiella sp.* strain BRL6−2. *Stand. Genomic Sci.* **2014**, *9*, 19.
(59) DeAngelis, K. M.; Sharma, D.; Varney, R.; Simmons, B. A.; Isern, N. G.; Markillie, L. M.; Nicora, C. D.; Norbeck, A. D.; Taylor, R. C.; Aldrich, J. T.; Robinson, E. W. Evidence supporting dissimilatory and assimilatory lignin degradation in *Enterobacter lignolyticus* SCF1. *Front. Microbiol.* **2013**, *4* (280), 1−14.
(60) Calusinska, M.; Marynowska, M.; Bertucci, M.; Untereiner, B.; Klimek, D.; Goux, X.; Sillam Dussès, D.; Gawron, P.; Halder, R.; Wilmes, P.; Ferrer, P.; Gerin, P.; Roisin, Y.; Delfosse, P. Integrative omics analysis of the termite gut system adaptation to *Miscanthus* diet identifies lignocellulose degradation enzymes. *Commu. Biol.* **2020**, *3*, 1−12.

https://dx.doi.org/10.1021/acssuschemeng.0c07817
ACS Sustainable Chem. Eng. 2021, 9, 2191−2202